Efficient Synergistic Immunotherapy for Inhibiting Tumor Postoperative Recurrence and Metastasis via Calcium Alginate Hydrogel Nanosystem

Tiange Wang
Tianjin University
Hanjie Wang (wanghj@tju.edu.cn)
Tianjin University
Yingying Zhang
Tianjin University
Tiandi He
Tianjin University
Xiaoli Wu
Tianjin University
Jin Chang
Tianjin University

Research

Keywords: tumor immunotherapy, synergistic immunotherapy, postoperative recurrence and metastasis, nanomaterials, calcium alginate hydrogel

Posted Date: December 6th, 2019

DOI: https://doi.org/10.21203/rs.2.18225/v1

Efficient Synergistic Immunotherapy for Inhibiting Tumor Postoperative Recurrence and Metastasis via Calcium Alginate Hydrogel Nanosystem

Tiange Wang[†], Hanjie Wang[†,], Yingying Zhang[†], Tiandi He[†], Xiaoli Wu[†],*

Jin Chang[†,]*

†School of Life Sciences, Tianjin University, Tianjin Engineering Center of Micro-Nano Biomaterials and Detection-Treatment Technology, 92 Weijin Road, Nankai District, Tianjin 300072, P.R. China

*Corresponding author: jinchang@tju.edu.cn and wanghj@tju.edu.cn

Abstract: Immunotherapy is expected to become an promising strategy in inhibiting tumor postoperative recurrence and metastasis. However, the effect is still unsatisfactory because of lacking cooperativity between various therapeutic methods. In this study, we designed an efficient synergistic immunotherapy system as an all-around and multi-dimension method for inhibiting tumor postoperative recurrence and metastasis. The efficient synergy lay in enhancing immune effect and eliminating immune suppression in the meantime by took advantages of CpG oligodeoxynucleotides (CpG ODNs) and antiPDL1 antibody. We introduced nanomaterials based on the calcium alginate hydrogel which has an acknowledged biological safety to implement the above strategy and make the system multifunctional. This nanosysterm have both therapy function and long-term monitoring capability *in vivo* to evaluate the recurrence and metastasis situation of postoperative residual tumor cells conveniently in real time. *In vitro and vivo* results proved that that this system could achieve a much better tumor inhibition efficiency and a good monitoring effect. This efficient synergistic immunotherapy nanosystem is expected to become a new promising strategy for postoperative immunotherapy of tumor.

Keywords: tumor immunotherapy; synergistic immunotherapy; postoperative recurrence and metastasis; nanomaterials; calcium alginate hydrogel

Background

Surgical resection is the most common choice to eliminate tumors in clinical at present[1, 2]. Postoperative recurrence and metastases often occurs along with it[3-6]. Therefore many people have aimed on develop strategies to prevent cancer recurrence and metastasis after surgery. Traditional methods such as chemotherapy or radiotherapy are often used to assist postoperative treatment[7-9]. But the effects of these traditional methods is still very limited and there are many defects of them include toxic side effects as well as drug resistance and so on. The failure of effectively inhibiting postoperative recurrence and metastasis is still the main reason make tumors difficult to cure. There is an urgent need to develop a long-term, systemic and high-security therapeutic strategy to solve this problem. In recent years, tumor immunotherapy has become a hot spot in the field of tumor therapy especially after surgery and the recent research has shown that using immunotherapy methods to assist surgical resection will become a promising strategy to inhibit tumor recurrence and metastasis in the postoperative treatment of tumors[10-13]. There are many available immunotherapy methods have been put into application at present[14, 15]. However, the effect is still unsatisfactory because of lacking cooperativity between various therapeutic methods so there is a urgent need to develop a synergistic strategy to obtain mutually reinforcing and enhanced therapeutic effect.

In this study, we designed an efficient synergistic immunotherapy system as an all-around and multi-dimension method for inhibiting tumor postoperative recurrence and metastasis. The efficient synergy lies in enhancing immune effect and eliminating

immune suppression in the meantime take advantage of CpG ODNs and antiPDL1 antibody. First, CpG ODNs is a single-stranded oligonucleotide fragment containing specific non-methylated CpG dinucleotide sequences[16-19]. It's a generally recognized Toll-like receptors (TLRs) agonists in recent years[20]. TLRs are expressed by most antigen presenting cells (APCs) such as dendritic cells (DCs), which is the most important class of APCs in the body. TLRs on DCs can sense a wide range of danger signals, which are conducive to the maturation of DCs. It is also contribute to stimulate the secretion of related cytokines and the maturation of cytotoxic T lymphocytes which can enhance the anticancer activity of various cancer treatment[21]. Second, immune checkpoint inhibitors have shown encouraging results in the treatment of various cancers[22]. In particular the antiPDL1 antibody, which is a key pathway to relieve the tumor inhibition of immune response[23-25]. This efficient synergistic immunotherapy system can promote the induction of persistent and specific anti-tumor T cell effects in vivo.

In recent years, nanomaterials have received wide attention in tumor immunotherapy because of its high efficiency drug delivery ability and multifunctional integration capability[26-28]. Therefore we introduced nanomaterials to implement the above strategy and gave the system more functionality. For inhibiting recurrence in situ, it was hoped that a smaller amount of CpG ODNs could produce sufficient immune effects. So we used the high biocompatibility injectable calcium alginate (CA) hydrogel to load CpG ODNs[29, 30]. Through the sustained release effect of hydrogel could improve the immune

activation effect of CpG ODNs. Furthermore, we also loaded the quantum dots-gold nanoparticles (QDs-AuNPs) probe based on the fluorescence resonance energy transfer (FRET) theory in the gel which can detect the content of a tumor marker carcinoembryonic antigen (CEA) in vivo[31]. CEA content reflected the level of tumor recurrence, so the tumor recurrence could be monitored in real time through the fluorescence signal of the probe which fixed in the tumor site. Then we used the same material to prepare calcium alginate nanoparticles as a carrier of antiPDL1 antibody which could improve the treatment effect rely on the advantages of nanomaterials to assist orthotopic therapy and inhibit the tumor metastasis. Meanwhile, ICG was loaded as imaging agent to diagnose tumor metastasis and drug aggregation. This nanosystem based on the calcium alginate hydrogels have both therapy function and long-term monitoring capability in vivo which could be injected into the body after surgical resection to inhibit tumor recurrence and metastasis. In the meanwhile, it could evaluate the recurrence and metastasis situation of postoperative residual tumor cells and the treatment effect conveniently in real time through the imaging testing.

A series of *in vitro* and *in vivo* experiments were conducted to test the effect of this nanosystem. We expected this efficient synergistic immunotherapy nanosystem could provide a new promising strategy for the postoperative immunotherapy of tumor.

Results

1. Calcium alginate hydrogel loads the CpG ODNs to enhance the immune effects through sustained release function.

First we aimed at using a sustained release strategy to attain a stronger immune effects by only adding a small quantity of CpG ODNs. We chose injectable calcium alginate hydrogel as the carrier to achieve our purpose which have a widely use and high biocompatibility. Sodium alginate and $CaCO_3$ were used to prepare the calcium alginate hydrogel, gluconolactone (GDL) was used to dissociate the Ca^{2+} from $CaCO_3$ then cross-linked with sodium alginate slowly (Figure 2a and Figure S1). It was liquid at first and will became solid after a while so it's a injectable hydrogel which is convenient to use (Figure S2). In order to acquire the suited calcium alginate hydrogel with long time fixation and sustained drug release function, we explored the preparation formula of our hydrogel based on the 2.5 % sodium alginate which is the commonly used percentage (Figure 2c). The percentage of $CaCO_3$ and GDL determine the solidification time of hydrogel. But if the percentage of GDL is too high, the PH of hydrogel will be too acidic to damage the tissue. After our exploration 8 % $CaCO_3$ and 8 % GDL were chose to prepare the hydrogel for next use and it had a relatively higher biosafety for cells (Figure S3). And use this preparation formulathe the hydrogel will become solid in about 5 minutes which is opportune enough to inject into the body and fix in situ rapidly. Then the CpG ODNs was loaded in the hydrogel and the release rate was test in a simulated physiological environment (37 ℃, PBS). It was proved that the CpG ODNs can sustained release in 24 hours (Figure 2d). The quantity of CpG ODNs we used (20 μg) was fewer then it be used alone in previous research (50 μg) because of the sustained release function of the hydrogel. We tested the therapeutic effect of our CA hydrogel loaded the small quantity CpG

ODNs in vivo (Figure 2e). The ELISA measurement of immune cytokines showed that our design can produce more stronger immune effect then used the CpG ODNs alone at the same condition (Figure 2f). The difference of the tumors growth between different groups also proves the CpG ODNs loaded in the alcium alginate hydrogel can obtain the enhanced therapeutic effect in inhibiting tumor postoperative recurrence through its sustained release function (Figure 2g) and had no effect on the health of the mice (Figure S5). The treatment principle was shown in Figure 2b.

2. CEA probe fixed by hydrogel in situ for monitoring the tumor recurrence.

Base on the therapy of CpG loaded in the CA hydrogel, we conceived of introducing a mechanism which is simple and easy to implement for monitoring the therapy result and the tumor recurrence situation in real time in vivo. To achieve this purpose we constructed the QDs-AuNPs probe based on the FRET theory (Figure 3a). The DNA aptamer1 and aptamer2 can conjugate to QDs and AuNPs respectively. The CEA aptamer on the one hand could connect the QDs and AuNPs then bring them closer together to achieve the FRET effect because of its two matched ends with aptamer1 and aptamer2 respectively. On the other hand the middle of the CEA aptamer could bond to CEA specifically so the FRET effect will disappear when there is any CEA exists.

The water-soluble and biocompatible glutathione-coated CdTe QDs was prepared by previous method with slight modification. The size of the QDs was about 5nm according to the results of transmission electron microscope and particle size analyzer (Figure 3c). The QDs can emit fluorescence at a wavelength of 650 nm under

the light excitation of 450 nm that could be used as a detect signal in vivo (Figure 3e). The AuNPs was prepared by the traditional crystal seed growth method. By adjusting the reaction parameters such as time and temperature we could prepare AuNPs which have light absorption at a wavelength cover around 650 nm that can be used for quenching the fluorescence of the QDs above mentioned (Figure 3e). The AuNPs we prepared had a regular shape and uniform size (Figure 3d). The aptamer connection was verified by agarose gel electrophoresis (Figure 3f) and the fluorescence quenching phenomenon prove the successful construction of CEA probe (Figure S6).

The efficacy of the probe was tested with different concentrations of CEA standard and used tumor cell culture media. There is a good linear trend of them for further applying (Figure 3g and 3h). We also verified the biosecurity of the probe (Figure S7). Then we loaded the probe in the hydrogel we prepared before and tested the detection efficacy. The fluorescence signal of the probe reflects the level of CEA content (Figure 3i). In sum, our recurrence monitoring mechanism showed a hopeful ability for further application and is expected to be a new detecting tool in vivo.

3. CANPs carried antiPDL1 antibody to assist orthotopic therapy for inhibiting the tumor recurrence and metastasis to achieve efficient synergistic immunotherapy.

Except the recurrence of tumor often occurs after surgery, the metastasis along with it also makes tumor difficult to cure. In order to assist orthotopic therapy and inhibit the tumor metastasis all over the body, we designed another nanosystem used calcium alginate hydrogel too. The synthesis method was shown in figure 4a. At first

we prepared calcium alginate nanoparticals (CANPs) used sodium alginate and $CaCl_2$. In the meantime we added ICG as an imaging agent in the preparation process. The ICG@CANPs have a uniform morphology (size are around 110 nm) and a good dispersion in water (Figure 4c). The good biosecurity is also be verified for further applying in vivo (Figure 4d). The CANPs is a good carrier because of there are plenty of carboxyl on it so it is easy to proceed surface modifying such as the reaction between carboxyl and amino which we used to conjugate the antiPDL1 antibody. In cell experiments we verified the conjugate result of antiPDL1 antibody on the ICG@CANPs and the combining capacity to tumor cells (Figure 4e). The ICG@CANPs with antiPDL1 group had stronger fluorescence then the group without antiPDL1 antibody after incubated with tumor cells for 2 hours. It showed that the ICG@CANPs with antiPDL1 antibody could block the PDL1 receptors on tumor cells effective. Next we inject this nanosystem into metastasis mouse models to verify the targeting ability to the tumor site in vivo (Figure 4f). After injected 3 h we could see conspicuous aggregation at lung metastases and liver metastasis compared with the control group. The CANPs carried antiPDL1 antibody could be further used to assist orthotopic therapy for inhibiting the tumor recurrence and metastasis to achieve efficient synergistic immunotherapy *in vivo* (Figure 4b).

4. The efficient synergistic immunotherapy nanosystem based on the calcium alginate hydrogel have both therapy function and long-term monitoring capability *in vivo* which could be injected into the body after surgical resection to inhibit tumor recurrence and metastasis and evaluate the inhibitting effect in

real time.

In order to further research whether our project has a good synergistic immunotherapy effect *in vivo*, the nanosystem was applied in Balb/c mice with subcutaneous and metastatic tumor model. The treatment process was simple described in figure 5a. We first performed surgical resection on tumor-bearing mice and left about 10 percent of the primary tumor tissue to simulate the case of incomplete resection in clinical. After the wound healed for two days, the mice in different groups were locally injected or intravenous injected different drug formulations. Including probe@CA+PBS (Group 1), probe@CA+freeCpG (Group 2), (probe+CpG)@CA (Group 3), probe@CA+CANPs (Group 4), probe@CA+CANPs-antiPDL1 (Group 5), (probe+CpG)@CA+CANPs-antiPDL1 (Group 6) (antiPDL1,10 ug. CpG, 20 μg). 24 hours after our treatment of different groups, we detected the content of $CD3^+CD8^+$ T cells in the lymph glands. The result displayed that the same amount of CpG loaded in the CA hydrogel could produce more $CD8^+$ tumor killing T cells (61.62 %) then it was free injected (45.21 %) (Figure 5b and 5c). In addition, our synergetic system as well as showed better immunological effect than use one immunotherapy method alone (73.83 %). We further detected the immune cytokine content after treatment in different stages (Figure 5d). Tumor recrudesce situation was monitored by measured the size of primary tumor every two days and used IVIS monitored the fluoresence alteration of the probe loaded in the CA hydrogel (Figure 5e and 5f). The inhibition effect of metastatic tumour in lung was displayed by pictures of lung tissue H&E stain sections (Figure 5g). All of the above

results showed that our efficient synergistic immunotherapy nanosystem could acquire a better therapeutic effect then other control groups and had no effect on the health of the mice (Figure S8 and S9). In particular it was more efficacious than only activating immune effect or only eliminated immune suppression which is often used previously in clinical.

Discussion

In this study, an efficient synergistic immunotherapy nanosystem based on calcium alginate hydrogel has been developed for inhibiting tumor postoperative recurrence and metastasis, leading to a good therapy function and long-term monitoring capability *in vivo* to inhibit tumor recurrence and metastasis and evaluate the inhibitting effect in real time as shown in Figure 1. Our results demonstrated that this system possesses great anti-tumor effect on 4T1 tumors. The nanosystem① first injected in situ of the tumor after surgery. The CpG loaded in the CA hydrogel can enhance the immune effect to kill the tumor cells. And the fluorescence signal of the probe which fixed in CA hydrogel could be detected to monitor the tumor recurrence by the probe in the real time. Then the nanosystem② was injected into the vein of the tail. The antiPDL1 antibody on CANPs can eliminate the immune suppression and facilitate T cell to kill the tumor cells. And the ICG loaded in CANPs can reveal whether there is a metastasis in the body through its fluorescence signal.

The safety of nanomaterials is important. The excellent biosafety of all nanomaterials we used was proved in the cytotoxicity studies *in vitro*. The body weight changes and the hematoxylin-eosin staining of the mouse's major organs

further proved the safety of our nanoparticles.

The efficient synergistic treatment strategies has attracted more and more attention in order to improve therapeutic effects. The main advantage of synergistic therapy is using smaller amounts of immunotherapy drugs to achieve a diversified immune effect and enhanced immune response. Meanwhile, the introduction of *in vivo* tumor monitoring mechanisms of our system may provide a new perspective for the integration of diagnosis and treatment in clinical.

Conclusions

In summary, we have successfully prepared an efficient synergistic immunotherapy nanosystem based on calcium alginate hydrogel for inhibiting tumor postoperative recurrence and metastasis. Among it the calcium alginate hydrogel loaded the CpG ODNs could enhance the immune effects through sustained release function and the CEA probe fixed by hydrogel in situ could monitor the therapy result and the tumor recurrence situation of postoperative residual tumor cells conveniently in real time *in vivo*. As for the CANPs with antiPDL1 antibody, it could assist orthotopic therapy for inhibiting the tumor recurrence and metastasis to achieve efficient synergistic immunotherapy. The results showed that the efficient synergistic immunotherapy nanosystem could achieve a much better tumor inhibition efficiency and a good monitoring effect through the imaging testing. This efficient synergistic immunotherapy nanosystem is expected to become a new promising strategy for the postoperative immunotherapy of tumor.

Methods

1. Materials

Sodium alginate (SA), Calcium carbonate ($CaCO_3$), Gluconic acid lactone (GDL), Cadmium chloride ($CdCl_2 \cdot 2H_2O$), L-Glutathione (L-GSH), Sodium hydroxide (NaOH), Sodium tellurite (Na_2TeO_3), cetyltrimethylammonium bromide (CTAB), Chloroauric acid ($HAuCl_4$), Silver nitrate ($AgNO_3$), Ascorbic acid, N-Hydroxysuccinimide (NHS), 1-(3-dimethylaminopropyl)-3-ethylcarbodiimide hydrochloride (EDC), Sodium chloride (NaCl), hydrochloric acid (HCl), Calcium chloride ($CaCl_2$), were obtained from Sigma-Aldrich (USA). Indocyanine green (ICG), Sodium dodecyl sulfate (SDS), Diethyl2,5-di(thiophen-2-yl)terephthalate (MES), 2-[4-(2-hydroxyethyl)piperazin-1-yl]ethanesulfonic acid (HEPES), Tris-Borate-EDTA (TBE), Tris(2-carboxyethyl)phosphine (TCEP), were got from Solarbio (China). CpG oligodeoxynucleotides (CpG ODNs) was obtained from Synbio. Aptamer1 (5'NH_2-AAAAAATTGAA), aptamer2 (CTGGTATAAAA-SH 3'), CEA aptamer (ATACCAGCTTATTCAATT), were obtained from Sagon (China). AntiPDL1 antibody was obtained from Bioxcell (USA).

2. Preparation of injectable calcium alginate hydrogel

The preparation method of injectable calcium alginate hydrogel is referred to the previous methods. First prepared the 2.5 % sodium alginate (SA) solution in reserve. Then added appropriate amount of $CaCO_3$ powder into the SA solution above mentioned to make the mass fraction of $CaCO_3$ is 4 %, 6 % and 8 % respectively. Finally added the GDL which compound is 4 % -16 % respectively. Mixed the

compound sufficient and it solidified after different times in different ratio.

3. Synthesis of the QDs and the AuNPs

The water-soluble and biocompatible glutathione-coated CdTe QDs was prepared by previous method with slight modification. Prepared 50 mL $CdCl_2 \cdot 2H_2O$ (6.5 mM) transferred to a round-bottom flask. Then added 0.2 g L-GSH to the flask and dissolved sufficiently. Used NaOH (1 mol/L) adjusted the PH to 8. Then heated the solution to 100 ℃. Rapidly added 40 mL Na_2TeO_3 (1.5 mM) and 10 mL $NaBH_4$ (0.25 M) in the flask. Maintained the temperature for the reaction. With the extension of reaction time, the emission wavelength of QDs we obtained will redshifted. The QDs was washed with deionized water for next application.

The synthetic method of AuNPs was referenced the traditional crystal seed induced growth method. Dissolved CTAB (0.2 M) and $HAuCl_4$ (0.5 mM) in 5 mL deionized water. Added 600 μL $NaBH_4$ (0.01 M) in it and vigorous stirring for 2 min at 25 ℃. The obtained crystal seed solution was used within two hours. Then dissolved CTAB (0.2 M) and $HAuCl_4$ (1 mM) in 5 mL ultrapure water and heated up to 77 ℃. Added 250 μL $AgNO_3$ (4 mM), 70 μL ascorbic acid (78.8 mM) in it and stirred evenly. Afterwards added 12 μL the above crystal seed solution and stirring for 20 min kept the speed and temperature. The AuNPs we obtained was washed with deionized water for next application.

4. Preparation of the CEA probe

The prepared ODs are rich in carboxyl because of the GSH on the surface. Activated the carboxyl for concatenating the aptamer1 with amidogen

(5'NH_2-AAAAAATTGAA). Take 10 mg ODs in the tube, dissolved with MES buffer (2 mL, 10 mM, PH=5.5). Added 1 mg EDC and 2.5 mg NHS then shook for 2 h at room temperature. After the reaction is completed, washed three times with ultrapure water. Then dissolved in HEPES buffer (2 mL, 10 mM, PH=7.2). Added 10 μL aptamer1 (100 μM) and shook slowly for 4 h at room temperature. Then washed three times with deionized water.

Utilized the sulfydryl on the AuNPs to conjugated the aptamer2 with sulfydryl (CTGGTATAAAA-SH 3'). The prepared AuNPs were washed up with deionized water then dissolved in 2% SDS solution (PH≈3). Take 2 mL AuNPs (5 mg/mL) in the tube. Added 10×TBE and NaCl maked the ultimately concentration was 1×TBE and 500 mM. Then added 10 μL aptamer2 which have been reducted with TCEP before. Shook slowly for 5 min at room temperature. Then washed three times with deionized water.

The CEA probe was prepared by mixed the ODs-aptamer1 (1 mg/mL), the AuNPs-aptamer2 (0.5 mg/mL) and the CEA aptamer (ATACCAGCTTATTCAATT, 1 μM) together then shook slowly for 30 min at 37℃.

5. Preparation of the nanosysterm①

Take 100 μL above probe and added appropriate amount of SA and $CaCO_3$ maked the concentration was 2.5 % and 0.8 % respectively. Then added 20 μg CpG ODNs and homogeneous mixed. At last added the GDL which concentration is 8 % finally.

6. Preparation of CANPs

Partially hydrolyzed the sodium alginate according to traditional method before used. Added 3 mL HCl (3 M) in 100 mL 1 % sodium alginate solution and heated up to 50 ℃ with reflux for 20 min. The product was centrifuged and collect the sediment. Resuspended the sediment with 100 mL HCl (0.3 M) and refluxed for 2 h. Then centrifuged and collected the sediment. Neutralized it with NaOH (1 M) and adjusted the pH to 2.85 with HCl (1 M). The soluble fraction was neutralized and added to 100 ml of ethanol. Centrifuged and collected the sediment. Added $CaCl_2$ (18 mM) dropwise in 0.06% (w/v) SA solution. Stirred for 1 h at room temperature.

7. Preparation of the nanosysterm②

Added 5 mg ICG in 5 mL CANPs solution (10 mg/mL) and stirred for 8 h. Washed with deionized water and collected the sediment. Used NHS and EDC activated the carboxyl of CANPs. Added 100 μg antiPDL1 antibody in the above CANPs and stirred for 12 h.

8. Cell culture and imaging

The 4T1 cell lines were maintained in high-glucose DMEM medium supplemented with 10 % FBS and 1 % penicillin/streptomycin mixture at 37 °C, 5% CO_2. For cell imaging, 2×10^5 cells were planted in a 12-well plate and put back to the incubator for 24 h. A fluorescence inversion microscope system (Olympus, Japan) with 808 nm laser was employed to achieve living cell imaging and the paraffin sections of organ H&E staining. Microscopy experiments were initiated after 4 h of incubation with our nanosystem. The imaging in vivo was used the caliper IVIS lumina II (Xenogen).

9. Mice experiments

Female BALB/C mice of 7-week old (Beijing Vital River Laboratory Animal Technology Co., Ltd) were used to do the animal experiments and were performed by the statutory requirements of People's Republic of China (GB14925-2010). When the primary tumors reached a volume of about 100 mm^3, the mice bearing tumor were performed the operation to resection the 90 % tumor. After two days for the wound healing we conduct the treatment. The detection of immune cells was used by FACS Calibur (BD). The detection of immune factor was used by ELISA (Solarbio).

10. Statistical analysis

Data analysis was performed by Excel and GraphPad Prism 6.01 software. For FCM significance analysis, the significance between two means was analyzed using an unpaired two-tailed t-test, and $P < 0.05$ was considered as significant (**$P < 0.01$). Every test was repeated at least for three times.

List of abbreviations

CpG oligodeoxynucleotides (CpG ODNs)

toll-like receptors (TLRs)

antigen presenting cells (APCs)

dendritic cells (DCs)

calcium alginate (CA)

carcinoembryonic antigen (CEA)

fluorescence resonance energy transfer (FRET)

gluconolactone (GDL)

calcium alginate nanoparticals (CANPs)

quantum dots (QDs)

gold nanoparticles (AuNPs)

Declarations

1. Consent for publication (Not applicable)

2. Availability of data and materials

The datasets used and/or analysed during the current study are available from the corresponding author on reasonable request.

3. Competing interests

The authors declare that they have no competing interests.

4. Funding

This work was sponsored by National Key Research and Development Program of China (2017YFA0205104), National Natural Science Foundation of China (31971300, 51573128, 51873150 and 81771970), Tianjin Development Program for Innovation and Entrepreneurship and Young Elite Scientists Sponsorship Program by Tianjin.

5. Authors' contributions

All authors took part in the writing process. All authors read and approved the final manuscript.

6. Acknowledgements

We thank the Laboratory Center of School of Life Sciences (Tianjin University)

for the flow cytometry instrument and School of Life Sciences (Nankai University) for the caliper IVIS lumina II.

References

[1]. Fields, R.C., et al., Surgical resection of the primary tumor is associated with increased long-term survival in patients with stage IV breast cancer after controlling for site of metastasis. Ann Surg Oncol, 2007. 14(12): p. 3345-51.

[2]. Pockaj, B.A., et al., Metastasectomy and surgical resection of the primary tumor in patients with stage IV breast cancer: time for a second look? Ann Surg Oncol, 2010. 17(9): p. 2419-26.

[3]. Zhang, Y., et al., Targeting of circulating hepatocellular carcinoma cells to prevent postoperative recurrence and metastasis. World J Gastroenterol, 2014. 20(1): p. 142-7.

[4]. Ceelen, W., P. Pattyn and M. Mareel, Surgery, wound healing, and metastasis: recent insights and clinical implications. Crit Rev Oncol Hematol, 2014. 89(1): p. 16-26.

[5]. Zhou, X.D., Recurrence and metastasis of hepatocellular carcinoma: progress and prospects. Hepatobiliary Pancreat Dis Int, 2002. 1(1): p. 35-41.

[6]. Tung-Ping, P.R., S.T. Fan and J. Wong, Risk factors, prevention, and management of postoperative recurrence after resection of hepatocellular carcinoma. Ann Surg, 2000. 232(1): p. 10-24.

[7]. Rutkowski, S., et al., Treatment of early childhood medulloblastoma by postoperative chemotherapy and deferred radiotherapy. Neuro Oncol, 2009. 11(2): p. 201-10.

[8]. Abaid, L.N., et al., Sequential chemotherapy and radiotherapy as sandwich therapy for the treatment of high risk endometrial cancer. J Gynecol Oncol, 2012. 23(1): p. 22-7.

[9]. Hejna, M., et al., Postoperative chemotherapy for gastric cancer. Oncologist, 2006. 11(2): p. 136-45.

[10]. Parfitt, J.R., et al., Primary PEComa of the bladder treated with primary excision and adjuvant interferon-alpha immunotherapy: a case report. BMC Urol, 2006. 6: p. 20.

[11]. Kieran, M.W., et al., Phase I study of gene-mediated cytotoxic immunotherapy with AdV-tk as adjuvant to surgery and radiation for pediatric malignant glioma and recurrent ependymoma. Neuro Oncol, 2019. 21(4): p. 537-546.

[12]. Park, C.G., et al., Extended release of perioperative immunotherapy prevents tumor recurrence and eliminates metastases. Sci Transl Med, 2018. 10(433).

[13]. Faries, M.B., et al., Long-Term Survival after Complete Surgical Resection and Adjuvant Immunotherapy for Distant Melanoma Metastases. Ann Surg Oncol, 2017. 24(13): p. 3991-4000.

[14]. Koo, G.C., et al., Immune enhancing effect of a growth hormone secretagogue. J Immunol, 2001. 166(6): p. 4195-201.

[15]. Motz, G.T. and G. Coukos, Deciphering and reversing tumor immune suppression. Immunity, 2013. 39(1): p. 61-73.

[16]. Wang, Z., et al., A bifunctional nanomodulator for boosting CpG-mediated cancer immunotherapy. Nanoscale, 2017. 9(37): p. 14236-14247.

[17]. Jahrsdorfer, B. and G.J. Weiner, CpG oligodeoxynucleotides for immune stimulation in cancer immunotherapy. Curr Opin Investig Drugs, 2003. 4(6): p. 686-90.

[18]. Shirota, H. and D.M. Klinman, Recent progress concerning CpG DNA and its use as a vaccine adjuvant. Expert Rev Vaccines, 2014. 13(2): p. 299-312.
[19]. Cerkovnik, P., et al., Tumor vaccine composed of C-class CpG oligodeoxynucleotides and irradiated tumor cells induces long-term antitumor immunity. BMC Immunol, 2010. 11: p. 45.
[20]. Murad, Y.M., et al., CPG-7909 (PF-3512676, ProMune): toll-like receptor-9 agonist in cancer therapy. Expert Opin Biol Ther, 2007. 7(8): p. 1257-66.
[21]. Gambuzza, M., et al., Targeting Toll-like receptors: emerging therapeutics for multiple sclerosis management. J Neuroimmunol, 2011. 239(1-2): p. 1-12.
[22]. Wilky, B.A., Immune checkpoint inhibitors: The linchpins of modern immunotherapy. Immunol Rev, 2019. 290(1): p. 6-23.
[23]. Blank, C. and A. Mackensen, Contribution of the PD-L1/PD-1 pathway to T-cell exhaustion: an update on implications for chronic infections and tumor evasion. Cancer Immunol Immunother, 2007. 56(5): p. 739-45.
[24]. Teng, F., et al., Progress and challenges of predictive biomarkers of anti PD-1/PD-L1 immunotherapy: A systematic review. Cancer Lett, 2018. 414: p. 166-173.
[25]. Mahoney, K.M., G.J. Freeman and D.F. McDermott, The Next Immune-Checkpoint Inhibitors: PD-1/PD-L1 Blockade in Melanoma. Clin Ther, 2015. 37(4): p. 764-82.
[26]. Sau, S., et al., Multifunctional nanoparticles for cancer immunotherapy: A groundbreaking approach for reprogramming malfunctioned tumor environment. J Control Release, 2018. 274: p. 24-34.
[27]. Xu, J., et al., Near-Infrared-Triggered Photodynamic Therapy with Multitasking Upconversion Nanoparticles in Combination with Checkpoint Blockade for Immunotherapy of Colorectal Cancer. ACS Nano, 2017. 11(5): p. 4463-4474.
[28]. Cheung, A.S., et al., Scaffolds that mimic antigen-presenting cells enable ex vivo expansion of primary T cells. Nat Biotechnol, 2018. 36(2): p. 160-169.
[29]. Zhao, L., M.D. Weir and H.H. Xu, An injectable calcium phosphate-alginate hydrogel-umbilical cord mesenchymal stem cell paste for bone tissue engineering. Biomaterials, 2010. 31(25): p. 6502-10.
[30]. Lee, K.W., et al., Sustained release of vascular endothelial growth factor from calcium-induced alginate hydrogels reinforced by heparin and chitosan. Transplant Proc, 2004. 36(8): p. 2464-5.
[31]. Li, X.H., et al., Hyperbranched rolling circle amplification (HRCA)-based fluorescence biosensor for ultrasensitive and specific detection of single-nucleotide polymorphism genotyping associated with the therapy of chronic hepatitis B virus infection. Talanta, 2019. 191: p. 277-282.

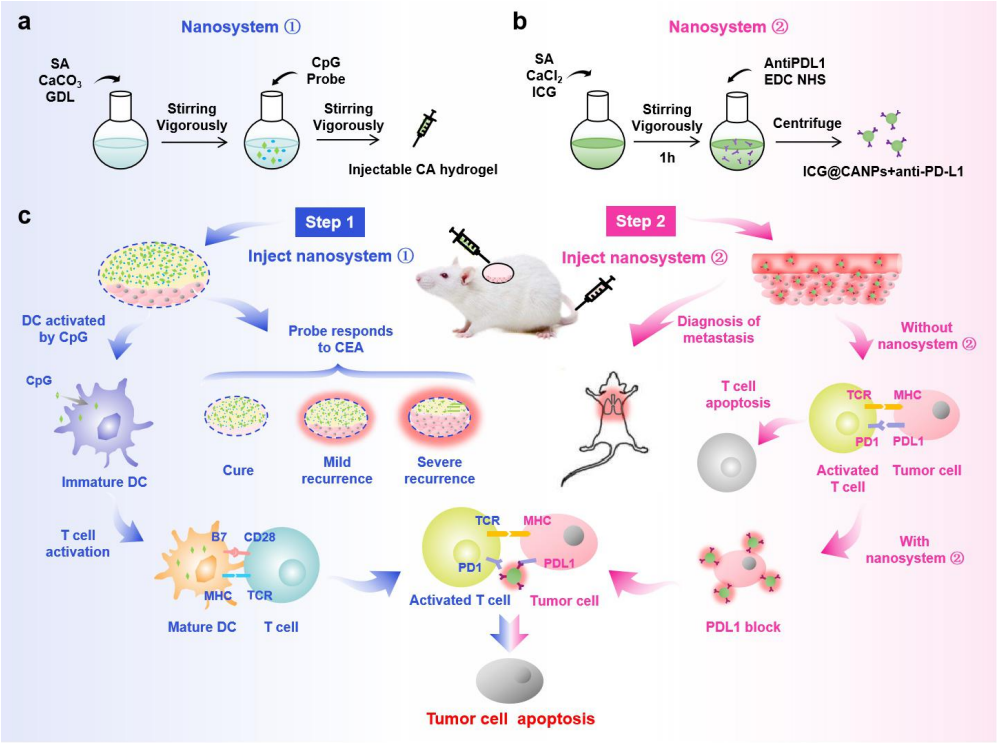

Figure 1. Schematic diagram of the efficient synergistic immunotherapy via calcium alginate hydrogel nanosystem for inhibiting tumor postoperative recurrence and metastasis in vivo. a) The preparation method of the injectable calcium alginate hydrogel loaded CpG and the CEA probe. b) The preparation method of the ICG@CANPs+antiPDL1 nanosystem. c) The therapeutic process of the efficient synergistic immunotherapy nanosystem. Step 1: Inject the nanosystem① in situ after surgery. The CpG loaded in the CA hydrogel can enhance the immune effect to kill the tumor cells. And the fluorescence signal of the probe which fixed in CA hydrogel could be detected to monitor the tumor recurrence by the probe in the real time. Step 2: Inject the nanosystem② into the vein of the tail. The antiPDL1 antibody on CANPs can eliminate the immune suppression and facilitate T cell to kill the tumor cells. And the ICG loaded in CANPs can reveal whether there is a metastasis in the body through its fluorescence signal.

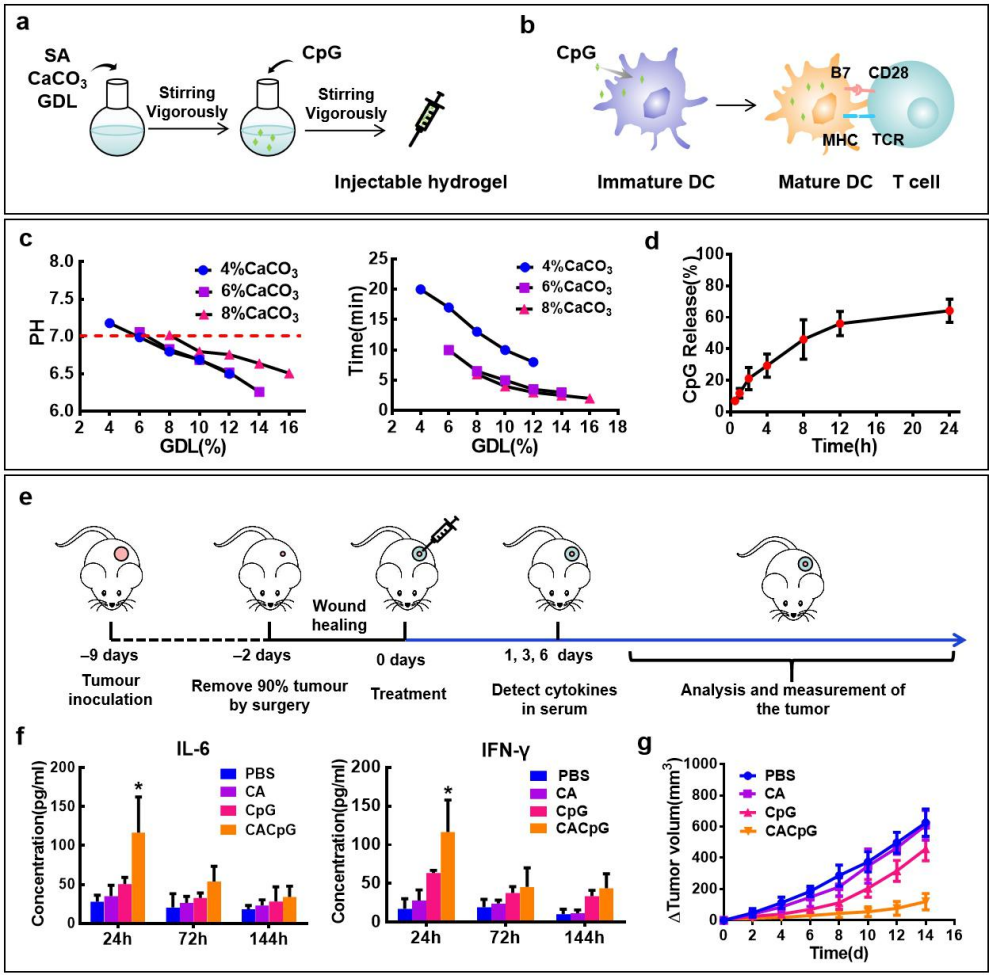

Figure 2. Calcium alginate hydrogel loads the CpG ODNs to enhance the immune effects through sustained release function. a) The preparation method of the injectable calcium alginate hydrogel loaded CpG. b) The treatment principle of CpG. c) The PH and coagulation time of the hydrogel with different percentage of $CaCO_3$ and GDL. The percentage of calcium alginate was 2.5 % in all experiment. d) The CpG release rate of the CpG@CA hydrogel at different times in PBS. e) The schematic diagram of the therapeutic process. f) The cytokines concentration of different groups. f) The tumor growth curve of different groups. n=3 from in vivo experiments. Error bars denote s.e.m. P value: *, $P < 0.05$.

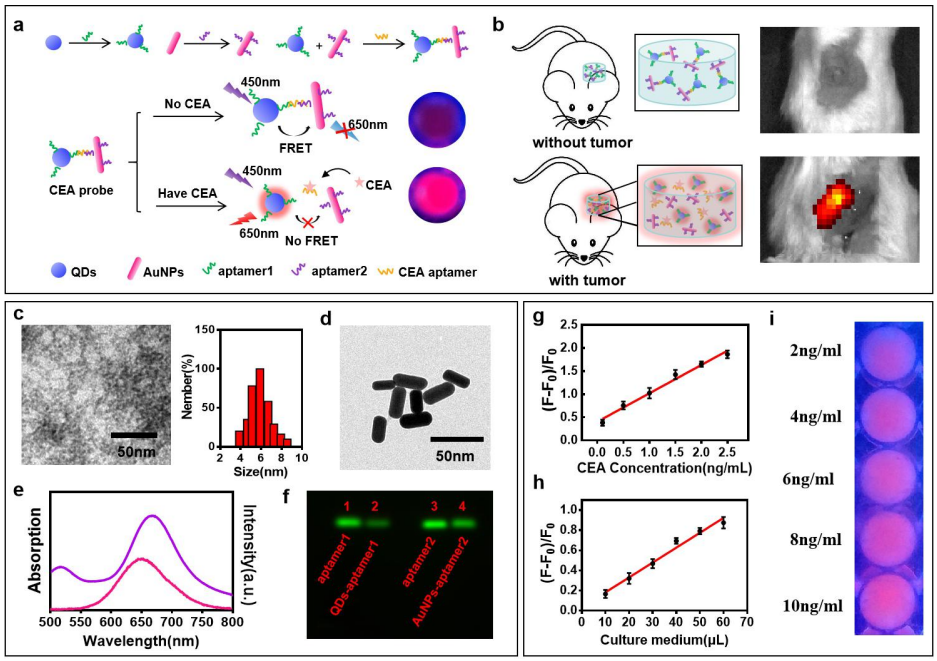

Figure 3. CEA probe fixed by hydrogel in situ for monitoring the tumor recurrence. a) Schematic diagram of the QDs-AuNPs probe we constructed based on the FRET theory. b) The monitoring principle of the CA hydrogel with CEA probe. c) The TEM picture and size column diagram of the QDs we prepared. d) The TEM picture of the AuNPs we prepared. e) The absorption spectrum of AuNPs (the purple curve) and the emission spectrum of QDs (the pink curve). f) The agarose gel electrophoresis picture of aptamer1, QDs-aptamer1, aptamer2 and AuNPs-aptamer2. All aptamers were labeled with the Cy3 dye. g) The detection standard curve of the QDs-AuNPs probe with CEA standards. Each sample was measured in triplicate. h) The detection standard curve of the QDs-AuNPs probe with used tumor cells culture medium. Each sample was measured in triplicate. i) The picture of CA hydrogel loaded probe in holes under ultraviolet rays. Different holes were added CEA solution with different concentration respectively.

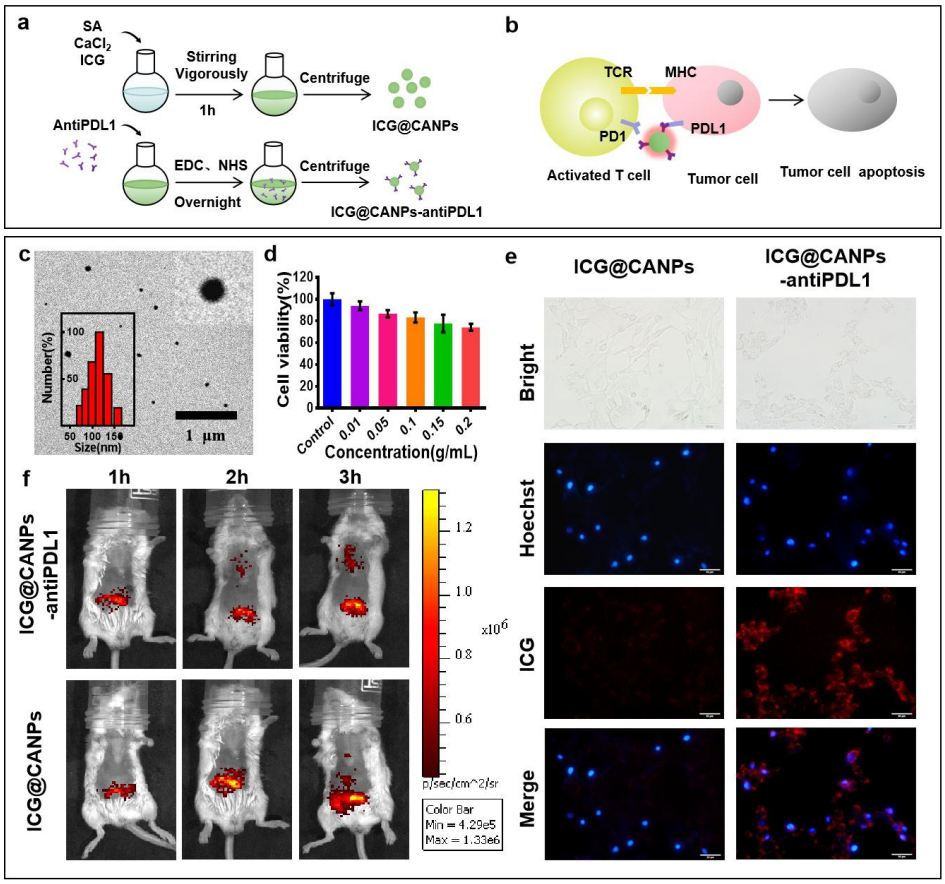

Figure 4. CANPs carried antiPDL1 antibody to assist orthotopic therapy for inhibiting the tumor recurrence and metastasis to achieve efficient synergistic immunotherapy. a) The synthetic method of ICG@CANPs-antiPDL1. b) The treatment principle of our nanosystem. c) The TEM picture and size column diagram of the CANPs we prepared. d) The cell viability of CANPs under different concentrations. Each group has five samples. e) The pictures of tumor cells incubation experiment by inverted fluorescence microscope (Scale bar: 50 μm). The red fluorescence of ICG loaded in the nanoparticles indicated the location of nanosystems. f) The pictures of metastasis mouse models after injected nanosysterms for different times by live animal imager. The red fluorescence of ICG loaded in the nanoparticles indicated the location of nanosystems.

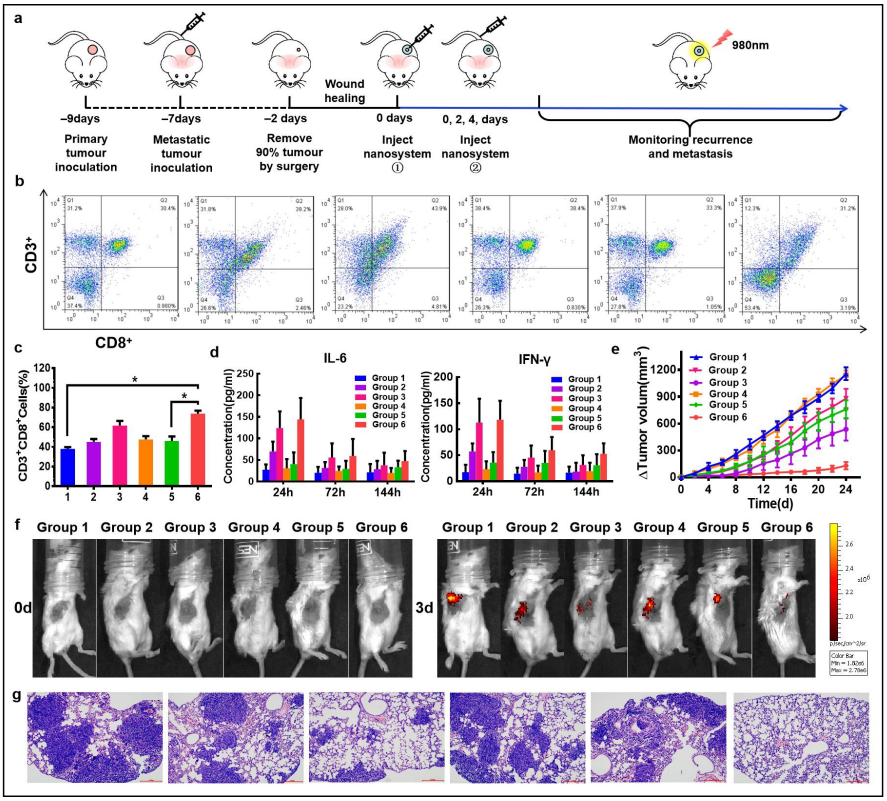

Figure 5. The efficient synergistic immunotherapy nanosystem used for inhibiting tumor recurrence and metastasis after surgical resection in vivo. a) The schematic diagram of treatment process in vivo. b) The flow cytometry result of $CD3^+CD8^+$ T cells in the lymph glands after different treatment of different groups. From left to right: Group 1, Group 2, Group 3, Group 4, Group 5, Group 6. c) Quantitative analyze of the $CD8^+$ T cells content ratio in entire T cells. d) The immune cytokine content of each groups after treatment in different stages detected by ELISA. e) The primary tumor growth volume of each groups in 24 days after traetment. f) The fluoresence alteration after treament of the probe loaded in the CA hydrogel which was injected in situ. g) Pictures of lung tissue H&E stain sections of each groups. The blue is the nodules of the lung tumor. From left to right: Group 1, Group 2, Group 3, Group 4, Group 5, Group 6. n=5 from in vivo experiments. Error bars denote s.e.m.

Supporting information

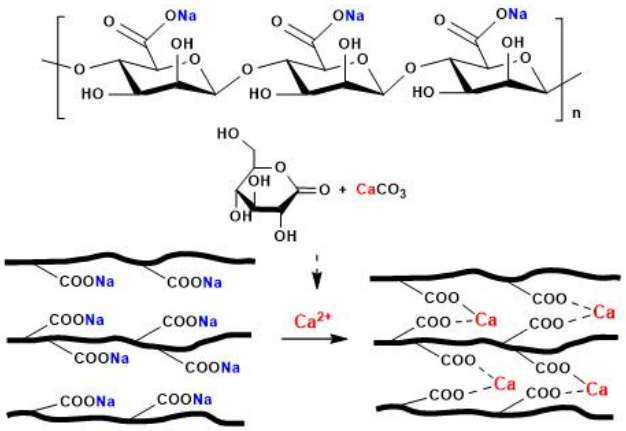

Figure S1. The formation principle of calcium alginate hydrogel.

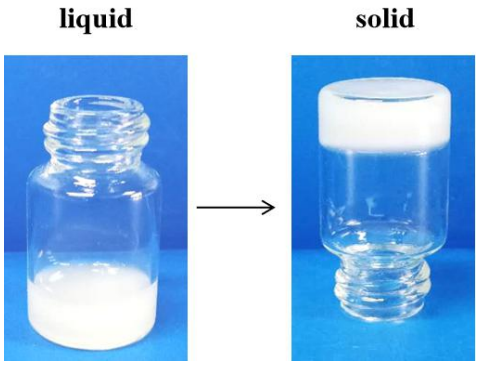

Figure S2. The pictures of sodium alginate mixed with $CaCO_3$ before added GDL and after.

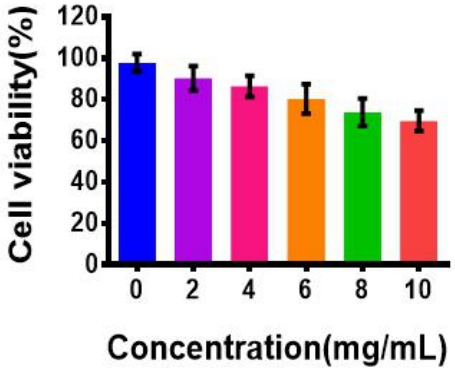

Figure S3. The biological security of calcium alginate hydrogel tested by MTT method.

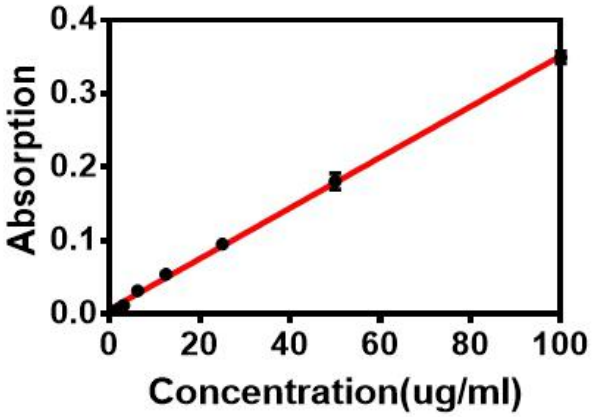

Figure S4. The ultraviolet absorption standard curve of CpG ODNs at 260 nm.

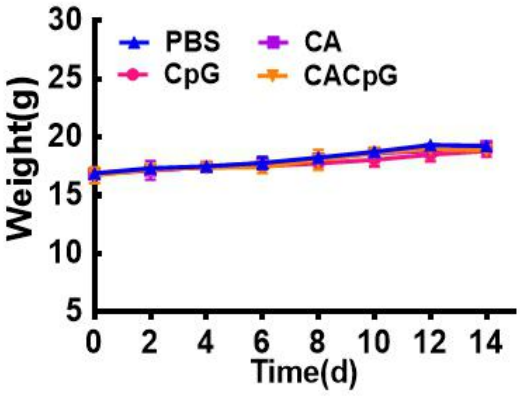

Figure S5. The weight of mice in different groups.

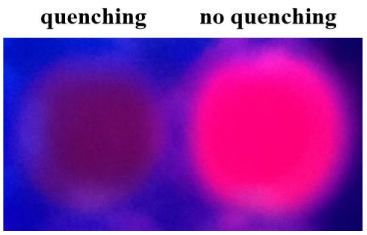

Figure S6. The picture under ultraviolet radiation of the QDs befor quenched by AuNPs and after.

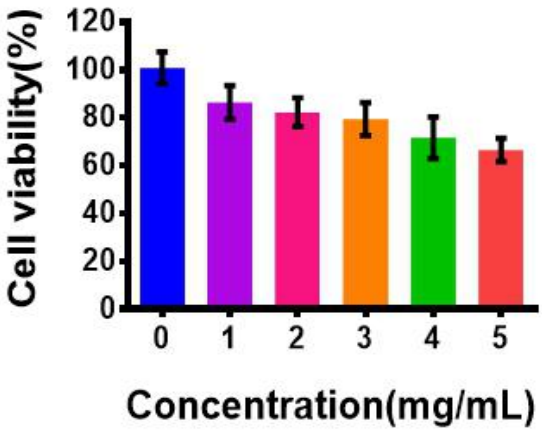

Figure S7. The biological security of CEA probe tested by MTT method.

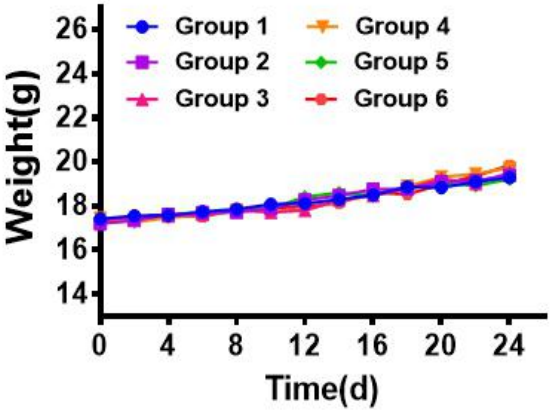

Figure S8. The weight of mice in each groups adopted different treatment.

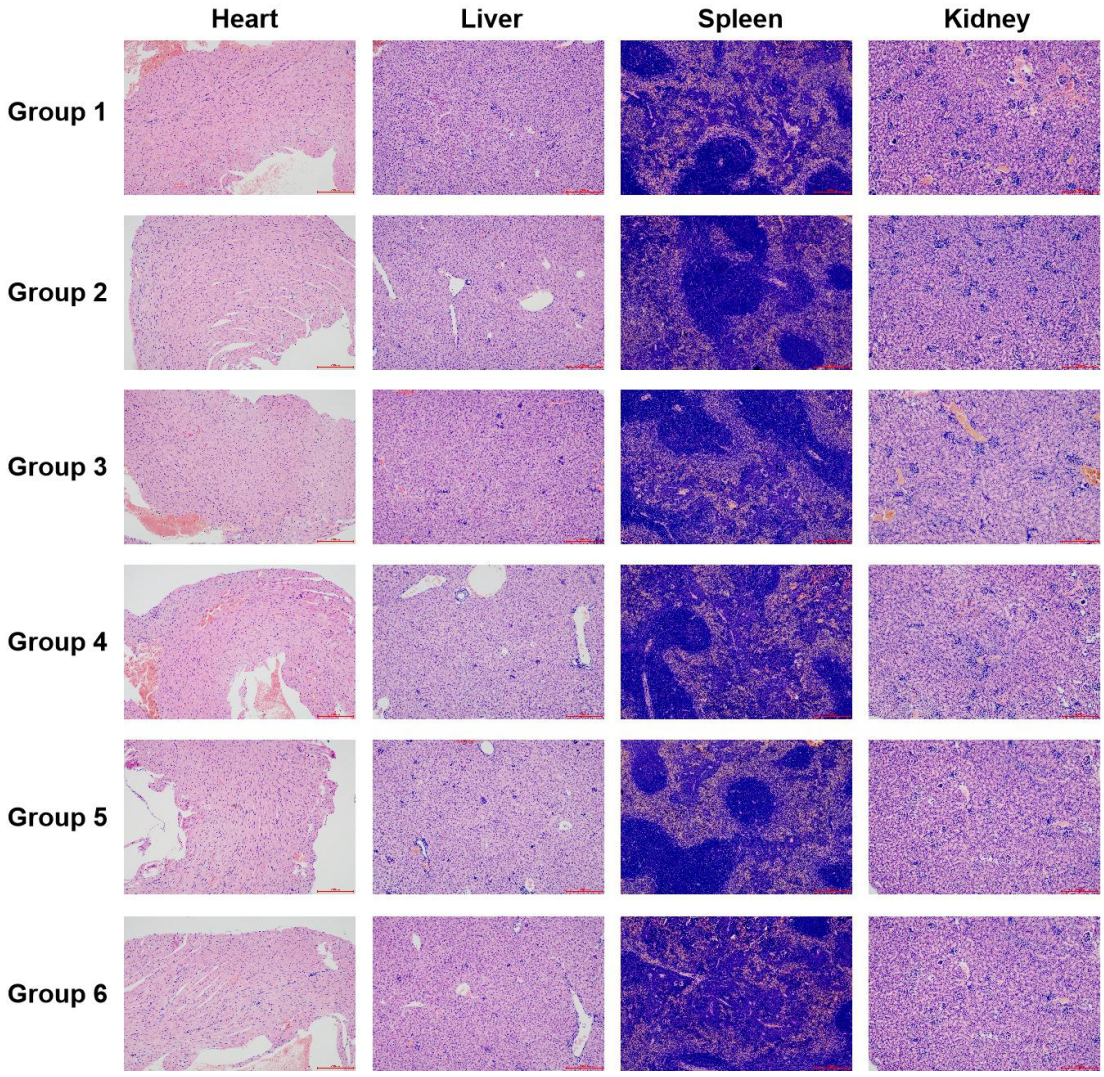

Figure S9. The pictures of vital organs H&E stain sections of mice in each groups adopted different treatment.

Figures

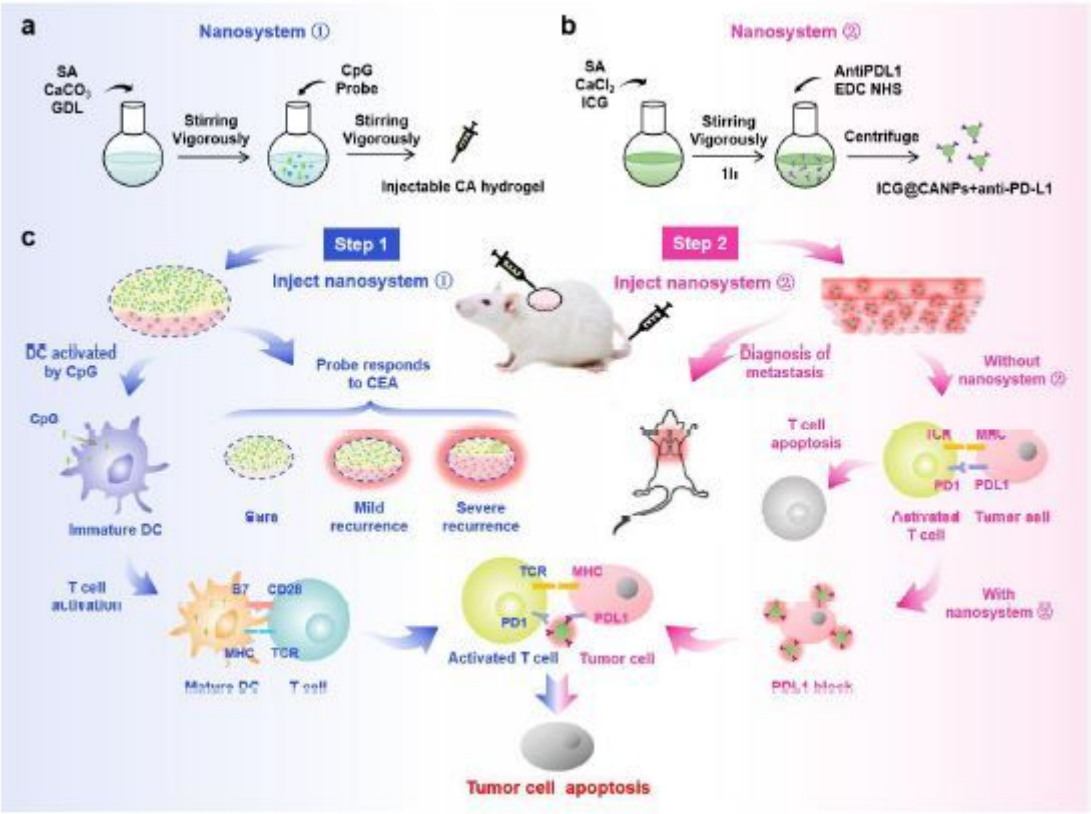

Figure 1

Schematic diagram of the efficient synergistic immunotherapy via calcium alginate hydrogel nanosystem for inhibiting tumor postoperative recurrence and metastasis in vivo. a) The preparation method of the injectable calcium alginate hydrogel loaded CpG and the CEA probe. b) The preparation method of the ICG@CANPs+antiPDL1 nanosystem. c) The therapeutic process of the efficient synergistic immunotherapy nanosystem. Step 1: Inject the nanosystem① in situ after surgery. The CpG loaded in the CA hydrogel can enhance the immune effect to kill the tumor cells. And the fluorescence signal of the probe which fixed in CA hydrogel could be detected to monitor the tumor recurrence by the probe in the real time. Step 2: Inject the nanosystem② into the vein of the tail. The antiPDL1 antibody on CANPs can eliminate the immune suppression and facilitate T cell to kill the tumor cells. And the ICG loaded in CANPs can reveal whether there is a metastasis in the body through its fluorescence signal.

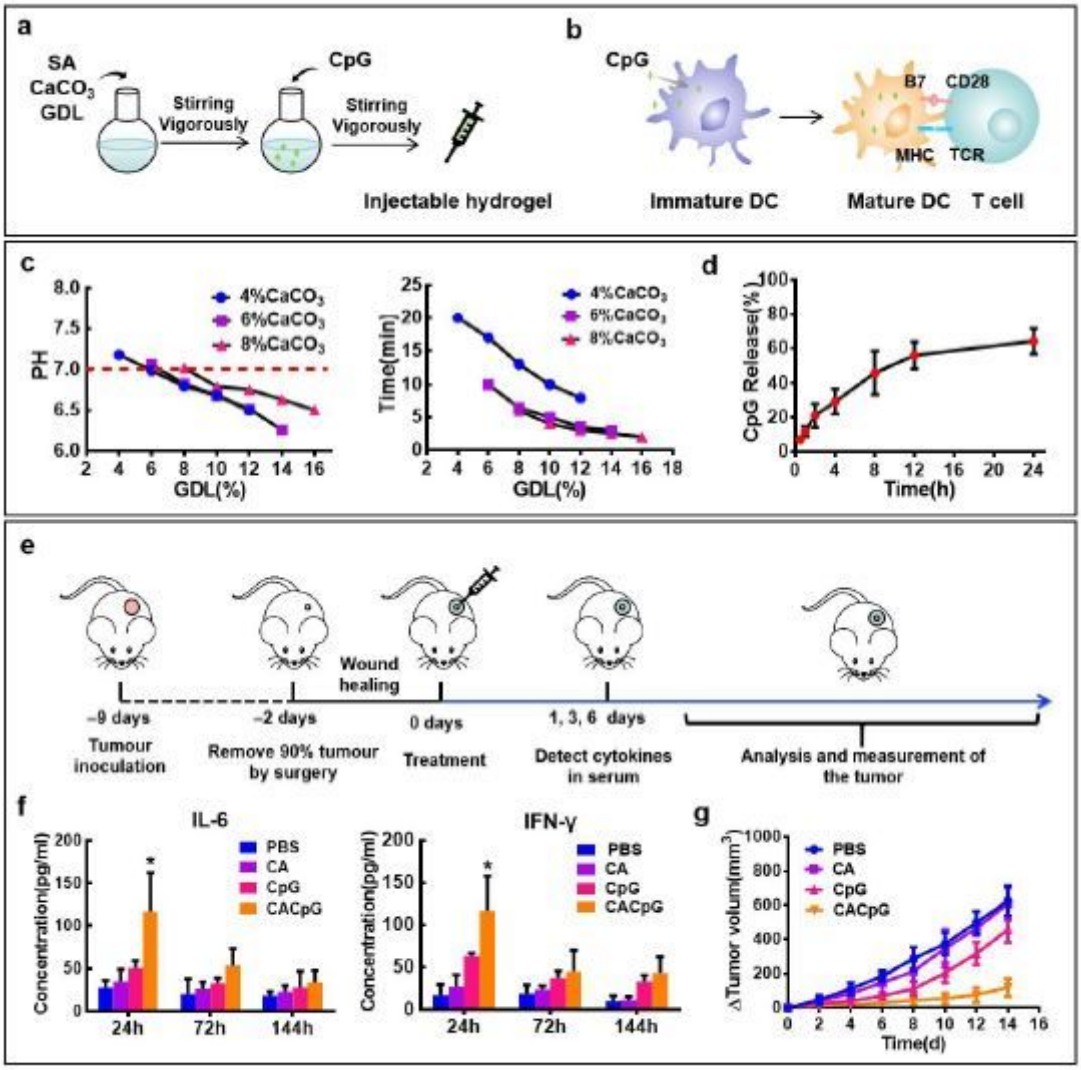

Figure 2

Calcium alginate hydrogel loads the CpG ODNs to enhance the immune effects through sustained release function. a) The preparation method of the injectable calcium alginate hydrogel loaded CpG. b) The treatment principle of CpG. c) The PH and coagulation time of the hydrogel with different percentage of CaCO3 and GDL. The percentage of calcium alginate was 2.5 % in all experiment. d) The CpG release rate of the CpG@CA hydrogel at different times in PBS. e) The schematic diagram of the therapeutic process. f) The cytokines concentration of different groups. f) The tumor growth curve of different groups. n=3 from in vivo experiments. Error bars denote s.e.m. P value: *, $P < 0.05$.

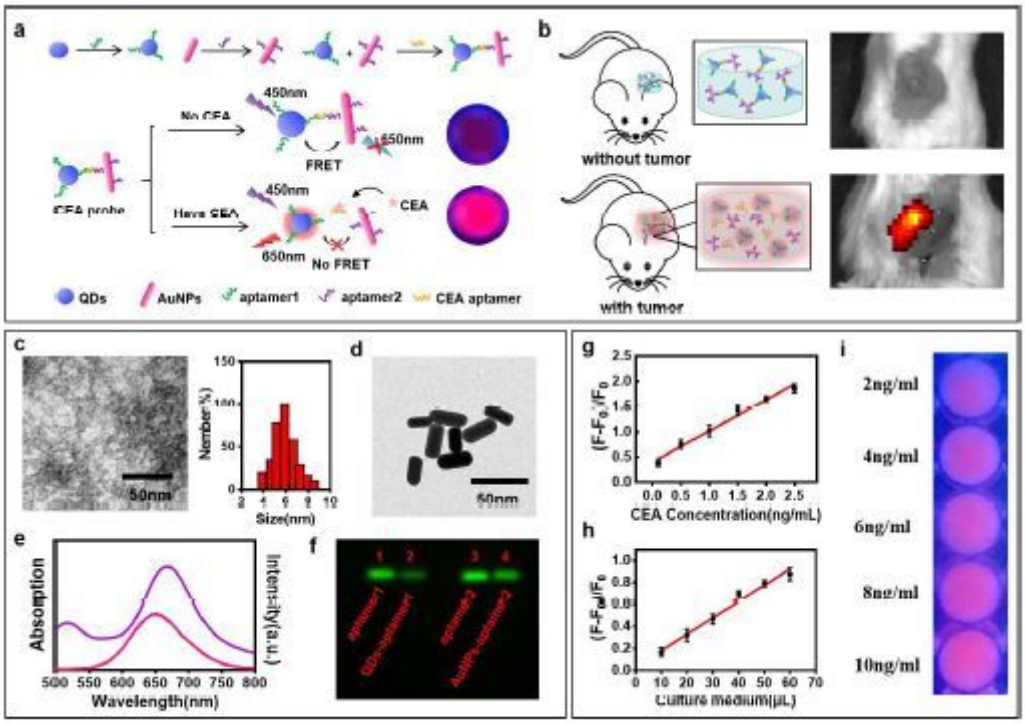

Figure 3

CEA probe fixed by hydrogel in situ for monitoring the tumor recurrence. a) Schematic diagram of the QDs-AuNPs probe we constructed based on the FRET theory. b) The monitoring principle of the CA hydrogel with CEA probe. c) The TEM picture and size column diagram of the QDs we prepared. d) The TEM picture of the AuNPs we prepared. e) The absorption spectrum of AuNPs (the purple curve) and the emission spectrum of QDs (the pink curve). f) The agarose gel electrophoresis picture of aptamer1, QDs-aptamer1, aptamer2 and AuNPs-aptamer2. All aptamers were labeled with the Cy3 dye. g) The detection standard curve of the QDs-AuNPs probe with CEA standards. Each sample was measured in triplicate. h) The detection standard curve of the QDs-AuNPs probe with used tumor cells culture medium. Each sample was measured in triplicate. i) The picture of CA hydrogel loaded probe in holes under ultraviolet rays. Different holes were added CEA solution with different concentration respectively.

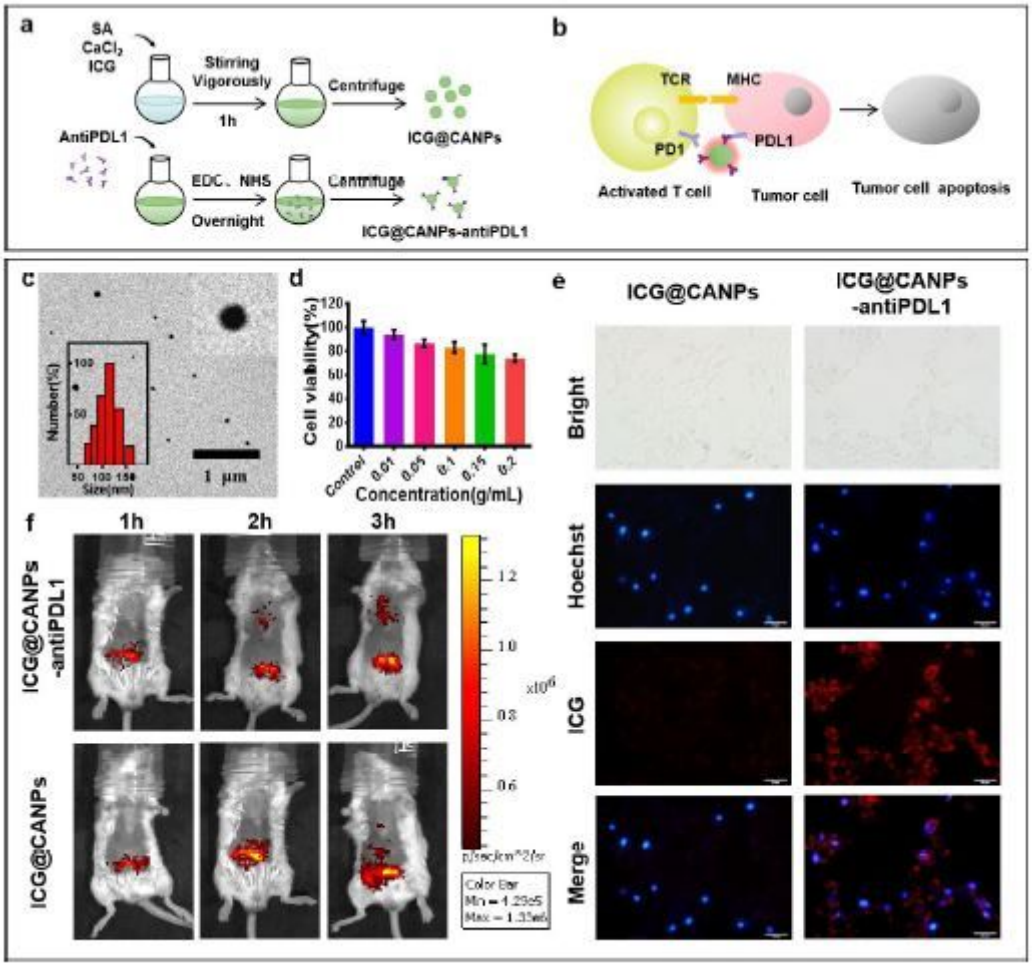

Figure 4

CANPs carried antiPDL1 antibody to assist orthotopic therapy for inhibiting the tumor recurrence and metastasis to achieve efficient synergistic immunotherapy. a) The synthetic method of ICG@CANPs-antiPDL1. b) The treatment principle of our nanosystem. c) The TEM picture and size column diagram of the CANPs we prepared. d) The cell viability of CANPs under different concentrations. Each group has five samples. e) The pictures of tumor cells incubation experiment by inverted fluorescence microscope (Scale bar: 50 μm). The red fluorescence of ICG loaded in the nanoparticles indicated the location of nanosystems. f) The pictures of metastasis mouse models after injected nanosysterms for different times by live animal imager. The red fluorescence of ICG loaded in the nanoparticles indicated the location of nanosystems.

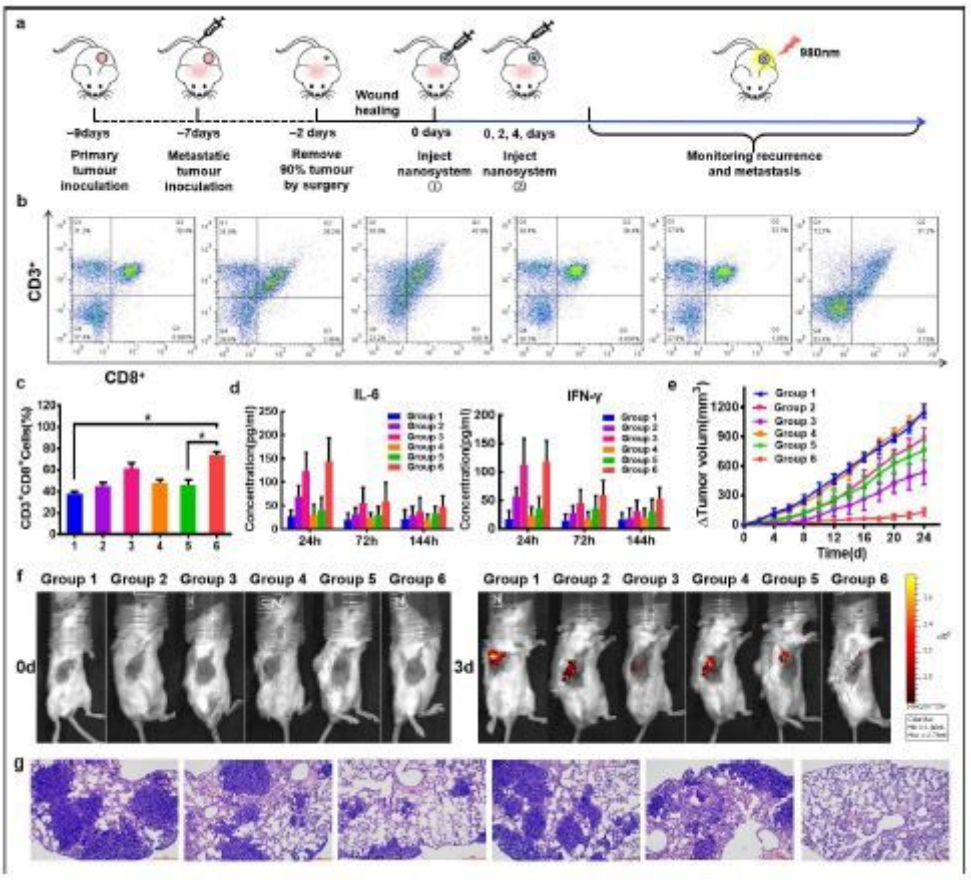

Figure 5

The efficient synergistic immunotherapy nanosystem used for inhibiting tumor recurrence and metastasis after surgical resection in vivo. a) The schematic diagram of treatment process in vivo. b) The flow cytometry result of CD3+CD8+ T cells in the lymph glands after different treatment of different groups. From left to right: Group 1, Group 2, Group 3, Group 4, Group 5, Group 6. c) Quantitative analyze of the CD8+ T cells content ratio in entire T cells. d) The immune cytokine content of each groups after treatment in different stages detected by ELISA. e) The primary tumor growth volume of each groups in 24 days after traetment. f) The fluoresence alteration after treament of the probe loaded in the CA hydrogel which was injected in situ. g) Pictures of lung tissue H&E stain sections of each groups. The blue is the nodules of the lung tumor. From left to right: Group 1, Group 2, Group 3, Group 4, Group 5, Group 6. n=5 from in vivo experiments. Error bars denote s.e.m.